SIMPLIFIED MODELLING AND NON-LINEAR ANALYSIS OF A HELICOPTER ROTOR IN VORTEX RING STATE

J.V.R. Prasad — Professor
Chang Chen — Graduate Student

School of Aerospace Engineering, Georgia Institute of Technology

Atlanta, GA, USA

P.-M. Basset — Senior Research Engineer
S. Kolb — Graduate Student

System Control and Flight Dynamics Department, ONERA

Salon-de-Provence, FRANCE

Nomenclature

C_Q	rotor torque coefficient, $Q/\rho\pi R^2(\Omega R)^2 R$
C_T	rotor thrust coefficient, $T/\rho\pi R^2(\Omega R)^2$
R	rotor radius, ft
T	rotor thrust, lb
V_i	rotor induced velocity, ft/s
V_Z	vehicle vertical speed, ft/s, positive in descent
VRS	vortex ring state
θ_o	collective pitch, deg
λ_i	non-dimensional induced velocity, $V_i/\Omega R$
λ_z	non-dimensional vertical speed, $V_Z/\Omega R$, positive in descent
ρ	air density, slug/ft^3
σ_e	equivalent rotor solidity
η	normalized climb rate, $-\lambda_z/\sqrt{C_T/2}$, positive in climb
ν	normalized induced inflow, $\lambda_i/\sqrt{C_T/2}$
Ω	rotor rotational speed, rad/s
DT0	collective pitch angle
DTC	lateral cyclic pitch control
DTS	longitudinal cyclic pitch control
DTA	tail rotor collective pitch angle
$P_{hel}, Q_{hel}, R_{hel}$	roll, pitch, yaw rates
$(U_{hel}, V_{hel}, W_{hel})$	helicopter velocity vector in the helicopter coordinate system
V_H	helicopter horizontal speed
Vi_h or Vi_0	main rotor mean inflow in hover
Vim_{MR}	main rotor mean induced velocity
Vim_{TR} or Vim_{Fan}	tail rotor mean induced velocity
(V_x, V_y, V_z)	helicopter velocity vector in the earth coordinate system
ϕ, θ	bank and pitch angles

Presented at the 30th European Rotorcraft Forum, Marseilles, France, September 14-16, 2004.

Abstract

This paper presents results from an on-going collaboration between ONERA and the Georgia Institute of Technology on Vortex Ring State (VRS) modelling, analysis and simulation. Specifically, validation of a previously developed 'Vortex Rings' model, which is capable of predicting rotor inflow behaviour in axial descent including the VRS, is presented. A methodology for the use of a VRS inflow model in the nonlinear analysis of the helicopter flight dynamic behaviour during descent flight is described. Results from an initial application of the method by bifurcation theory, are compared with flight test data in the prediction of the VRS boundaries.

Introduction

A helicopter is able to stay aloft in the air because its rotor pushes the air downwards and generates an upward thrust to balance the rotorcraft weight. When a helicopter increases its sink rate, especially when its sink rate is close to the rotor induced velocity, the rotor enters its own wake and creates a doughnut-shaped ring, known as the Vortex Ring State (VRS). Flight in VRS condition can be dangerous as it may result in excessive unsteady blade loads, thrust and torque fluctuations, vibration, unsteady heave dynamics, and loss of control effectiveness.

Within a French / US MoA task dedicated to rotorcraft flight dynamics, a cooperation between ONERA and the Georgia Institute of Technology has been established. The activity is first focused on the VRS problem as a continuation of their previous work (Ref. 1) on this topic. Beyond the modelling problem, a methodology is set up to use mathematical tools like bifurcation theory which are able to provide a more comprehensive understanding of non-linear system dynamics. Indeed, in some areas of the rotorcraft flight envelop, the non-linear terms in the dynamic equations become predominant. That is the case of the flight dynamics in the VRS.

The paper is arranged in two parts. The first part describes rotor inflow modelling in the VRS and validation using windtunnel test data. The second part describes a methodology for bifurcation analysis of rotorcraft flight dynamics in the VRS.

Part 1 : Rotor Inflow Modelling in the VRS

Castles and Gray (Ref. 2) performed wind-tunnel tests of rotors operating in the VRS. Four rotor configurations were examined in order to investigate the influence of blade twist, blade taper, rotor thrust coefficient, rotor speed, and rotor diameter. Variations of induced velocity, collective pitch, and torque coefficient were studied at different descent rates (wind-tunnel fan speed). Significant influence of twist was described while impacts from thrust coefficient, rotor speed, or rotor diameter were found negligible.

In order to analytically predict the VRS boundaries, Wolkovitch (Ref. 3) assumed that the slipstream was surrounded by a protective tube of vorticity in descent and concluded that VRS would occur when the flow at the core of the tube was zero.

Wang (Ref. 4) attempted to apply classical vortex theory in vertical descent. Instead of the conservation of circulation in an ideal flow, Wang assumed a linear decay of circulation of trailing vortices, typical of a real wake. The distance required for the linear decay (down to zero) was further assumed to be directly proportional to the transport velocity of trailing vortices. The direction of vortex shedding depended on the direction of the transport velocity. With appropriate selection of a few parameters, Wang was able to show good correlation between induced velocity and descent rate, as compared with the experimental data from (Ref. 2).

A significant development of VRS study in recent years was the time-accurate free-vortex wake scheme initiated by Leishman and Bhagwat (Ref. 5). The aerodynamics phenomenon associated with descending flight is described as follows: In hover and at low descent rates, the rotor wake is inherently unstable. As descent rate increases, the wake is more prone to be unstable and regular helical structure of the wake tends to break down. As net velocity near the rotor becomes low at higher descent rates, vorticity accumulates near the rotor plane and individual tip vortices form tight bundles of vorticity resembling vortex rings. These rings are found to be spatially and temporally unstable, and break away from the rotor disk, resulting in the fluctuations of blade loads and rotor thrust.

The free-vortex wake approach in (Ref. 5) offers a better understanding of the initiation and subsequent development of VRS through detailed computation of the flow behaviour. Nevertheless, it is also realised that this approach is computationally expensive and has inherent difficulties in integrating it with current helicopter flight simulation models.

Momentum theory has been widely used in hover, climb, and even forward flight conditions for flight mechanics analyses and flight simulation. It has also been recognised that the theory breaks down in descent flight due to the collapse of smooth slipstream. Nevertheless, rotorcraft researchers have developed various methods in extending the momentum theory in descending condition due to its simplicity. One of the earliest efforts can be traced back to Glauert in 1926 (Ref. 6). Recent attempts were from He, Lee and Chen (Ref. 7) and ONERA (Ref. 8-9). They individually formulated parametric extension of the momentum theory in the flow model to remove the modelling singularity in VRS and rendered simulation models covering the full range of flight conditions. Also,

ONERA performed a flight test campaign dedicated to the VRS using a Dauphin helicopter (Refs. 10-11).

Perhaps the most comprehensive parametric extension of the momentum theory was from Johnson (Ref. 12). A broad review of available wind tunnel and flight test data was conducted for rotors in VRS. Based on the available data, a VRS model was developed suitable for simple calculations and for real-time simulations. With this VRS model, Ref. 12 showed negative (unstable) heave damping for certain range of descent rates and the VRS boundaries were thus defined in terms of the stability boundary of the aircraft flight dynamics.

A new simplified inflow model called the 'Vortex Rings' model was developed in (Ref. 13) to account for the additional induced inflow at the rotor due to rotor-wake interaction during axial flight. The inflow model of Ref. 13 assumes slipstream in the rotor centre with a series of vortex rings located at the rotor periphery. All those vortex rings induce additional downward velocities at the rotor disk. The summation of these additional velocities and the original induced velocity (obtained from the momentum theory) provides an improvement in predicting the inflow at the rotor disk in descent flight.

The present work considers validation of the vortex rings model using the wind-tunnel experimental data of Ref. 2. First a brief description of the vortex rings model is given. This is followed by model validation results.

A Simplified Rotor Inflow Model for Vertical Descent

As pointed out in Ref. 13, one of the reasons for the under-prediction of induced velocity by the momentum theory is the ignorance of the interaction between the rotor, its wake and the surrounding airflow. The interaction may be less significant at hover or in climb. Nevertheless, it becomes more and more intense as a helicopter increases its descent rate due to larger velocity gradients between the upflow outside the wake and the downflow inside the wake.

The vortex rings model assumes slipstream in the rotor centre with a series of vortex rings located at rotor periphery. The formation of a vortex ring is caused by the aerodynamic interaction. A vortex ring moves downward along the wake at low descent rates (see Fig. 1a), or accumulates at the blade tip at moderate descent rates (when the total velocity at the blade tip is close to zero, see Fig. 1b), or moves upward along the wake at high descent rates (see Fig. 1c). After a blade rotation of 2π radians, a new vortex ring is formed. Therefore, at every instant, there are a series of discrete vortex rings along the wake and their locations are determined by the product of total velocity at the blade tip and time to travel across the azimuth of $2\pi m/\Omega$ (m: an integer). All these vortex rings induce additional downward velocities at the rotor disk (Ref. 14). The summation of these additional velocities and the original induced velocity (obtained from the momentum theory) provides an improvement in predicting the inflow at the rotor disk in descent flight.

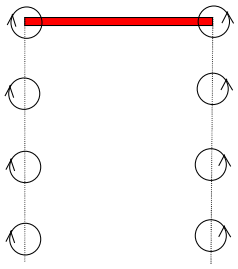

Figure 1a : Motion of Vortex Rings at Hover and Slow Descent.

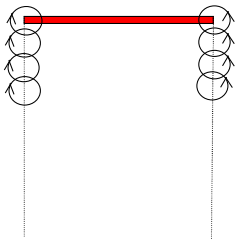

Figure 1b : Motion of Vortex Rings at Moderate Descent Rate.

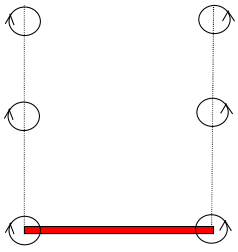

Figure 1c : Motion of Vortex Rings at High Descent Rate.

An important issue is to decide the strength of vortex rings. As the vortex ring is formed by the aerodynamic interaction at the blade tip, the strength of a vortex ring is proportional to the

velocity gradient at that location. Although it is still difficult to determine the exact value of the strength, it can be compensated by selecting proper number of vortex rings to correlate with experimental data. The number has significant impact on the add-on portion of induced velocities when the vortex rings accumulate at moderate descent rates. In the subsequent validation, the nominal number is set at 4. The actual number can be varied in a pre-defined range. In fact, the uncertainty of the number reflects the reality where the rings in VRS condition may burst in a random fashion. This indeed provides a numerical means of randomness in the distribution of induced velocity and hence, the thrust coefficient.

The vortex rings model is implemented in the generic rotorcraft flight simulation code FLIGHTLAB (Ref. 15). With the vortex rings model, additional downward velocities are achieved along both helicopter and windmill branches. According to Ref. 13, the transition between these two branches can be initiated through reduction in collective pitch during full-vehicle dynamic response simulation. The dynamic process essentially forces the total inflow to change its sign, hence the switch between two steady state solutions. This corresponds to the migration between two domains of attraction in the nonlinear system analysis. The suggested dynamic response is consistent with the pilot's experience when he/she lowers the collective control lever to *flat pitch* in order to enter into autorotation.

With the modification to induced velocity, the collective pitch needed for a descent rate is different. Especially at moderate descent rates (η roughly from -0.5 to -1.5), the increase in induced velocity from the vortex rings model reduces the effective blade angle of attack, and thus requires a larger collective pitch to balance the vehicle weight. Thus, higher collective pitch may be required to increase the rate of descent. By the same token, larger values of rotor torque can also be observed at moderate descent rates.

With the vortex rings' model, there is not only an additional component of induced velocity beyond what is predicted by the momentum theory, but also a steeper and varying gradient of the ν-η curve. This indicates that the increase of induced velocity is more rapid than the increase of descent rate. The direct impact of the steeper gradient is the change of the sign of heave damping at certain descent rates, as shown in (Refs. 12, 13).

Model Validation

The wind tunnel experimental data presented in Ref. 2 is used in the vortex rings model validation. The validation results presented are for the nominal rotor configuration used in Ref. 2, *i.e.*, constant chord and no blade twist.

Modelling and Froude Scaling

The baseline wind-tunnel model in Ref. 2 is a three-bladed, 3-foot radius rotor with an effective solidity of 0.05. The constant chord, untwisted blade has NACA 0015 airfoil section. The nominal rotational speed is 1200 RPM.

During the modelling process and simulation evaluations using the Flightlab, it is found that there are a few disadvantages if the original size of the rotor model is adopted. First, the rotor rotational speed is excessive as compared with that of a typical full-size rotor. It requires a very fine time step, which may cause numerical problems in the simulation. Second, the tip velocity of the blade (377 ft/sec) is smaller than that of a typical full-size helicopter rotor by nearly a factor of 2. This brings a suitability issue in the application of existing aerodynamics look-up tables in FLIGHTLB, as they are more applicable for higher Reynolds number. Third, the values of airframe moments of inertia are so small that it may introduce numerical inaccuracy for the subsequent full vehicle dynamic response simulation.

As such, Froude scaling scheme is adopted to enhance numerical reliability of the simulation. In this modelling, the Froude Scale number is set at 3. This will bring the scaled rotor tip velocity to 650 ft/sec.

Induced Velocity Variation along Helicopter and Windmill Branches

Variation of normalised induced velocities from the vortex rings model is shown in Figure 2a. The prediction from momentum theory and results from the wind-tunnel tests of Ref. 2 are also shown in the figure. Simulation was conducted under two different C_T: 0.002 and 0.004. Two observations can be made from Figure 2a. First, the calculated induced velocity variation from the vortex rings model captures the right magnitude as compared with the experimental data. If the number of vortex rings is varied in a small range, a fluctuation pattern of induced velocities can be created (see Figure 8 in Ref. 13). Second, there is no significant difference in the normalised induced velocity distribution due to variations in the thrust

coefficient. This observation is consistent with the conclusion from Ref. 2.

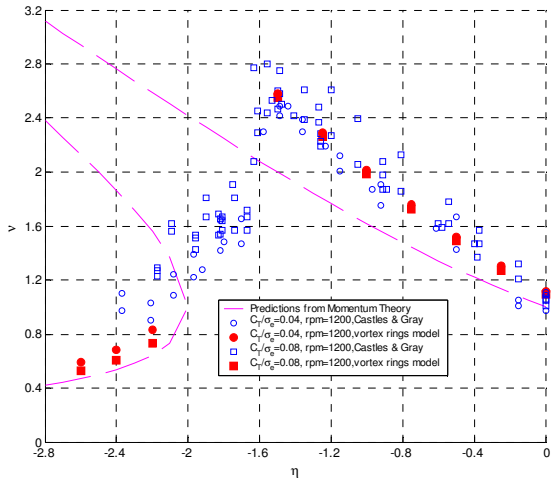

Figure 2a : Variation of Induced Velocity along Helicopter & Windmill Branches.

Collective Pitch Variation along Helicopter and Windmill Branches

The collective pitch variation with respect to vertical descent rate is shown in Figure 2b. Notice that from hover to roughly η=-1.5, the collective pitch predicted by the vortex rings model is almost constant, the same trend revealed by the experimental data. This reflects the fact that the add-on downward velocity induced by the vortex rings reduces the blade angle of attack and requires to maintain or even slightly increase the collective pitch for the purpose of trimming.

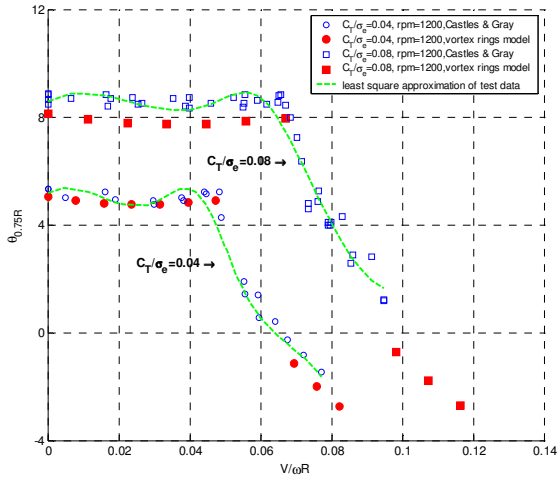

Figure 2b : Collective Pitch Variation along Helicopter & Windmill Branches.

Torque Coefficient Variation along Helicopter and Windmill Branches

The torque coefficient variation is presented in Figure 2c, which shows good agreement between the prediction from the vortex rings model and experimental data. These results highlight the important inclusion of the add-on downward velocity in rotor power prediction.

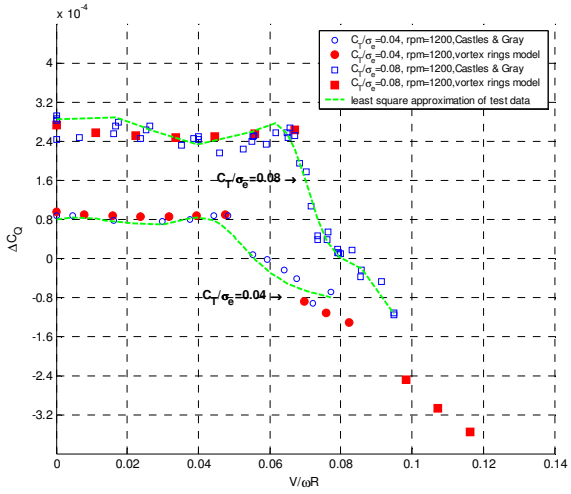

Figure 2c : Torque Coefficient Variation along Helicopter & Windmill Branches.

Transition

The steady state results described above are mainly obtained along the helicopter and the windmill branches. As mentioned before, the transition phase can be initiated by collective pitch reduction in full-vehicle dynamic response simulation.

The reduction profile of collective pitch used in this study is shown in Figure 3a. The collective pitch is initially decreased gradually, as shown in the first three gentle reductions. A large decrease occurs at approximately 53 seconds into the simulation, after which the collective pitch remains unchanged. The corresponding vertical descent rate is presented in Figure 3b.

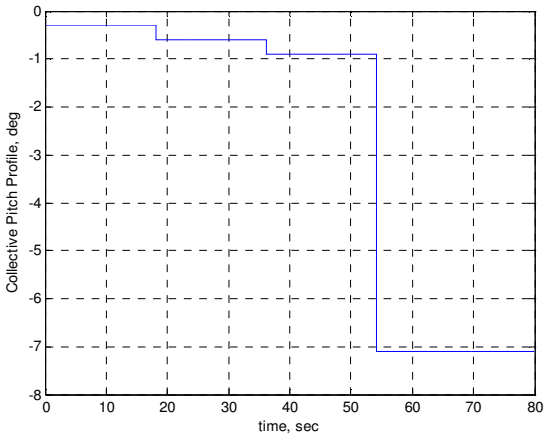

Figure 3a : Collective Control Reduction Profile for Dynamic Response.

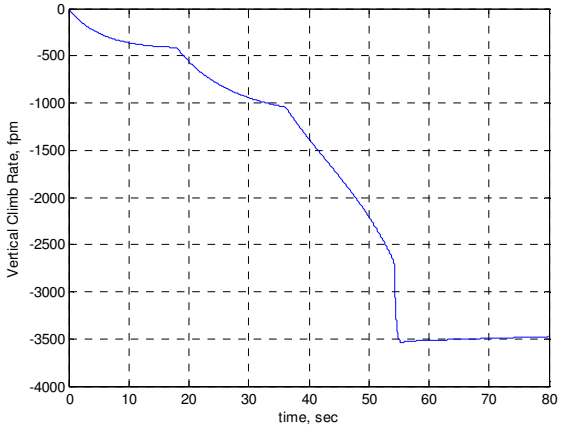

Figure 3b : Time History of Vertical Descent Rate for Dynamic Response.

During the first two mild reductions of collective pitch, the descent rate decreases moderately. However, there is a rapid drop in the descent rate during the third mild reduction, indicating the presence of unsteady heave dynamics. During the process, the total velocity at blade tip decreases rapidly. When it is close to zero speed, it triggers the need for a large reduction in collective pitch. The amount of reduction corresponds to the collective pitch difference between the steady state values at η=-1.5 and η=-2.0. At the final stage of dynamic simulation, the descent rate reaches a steady value, roughly η=-2.0.

The variation of normalised induced velocity versus vertical descent rate is shown in Figure 3c. The presence of a transition between helicopter and windmill branches is clear. Also, indications of transition are seen in Figures 3d and 3e in which both total inflow and torque coefficient change sign after transition occurs.

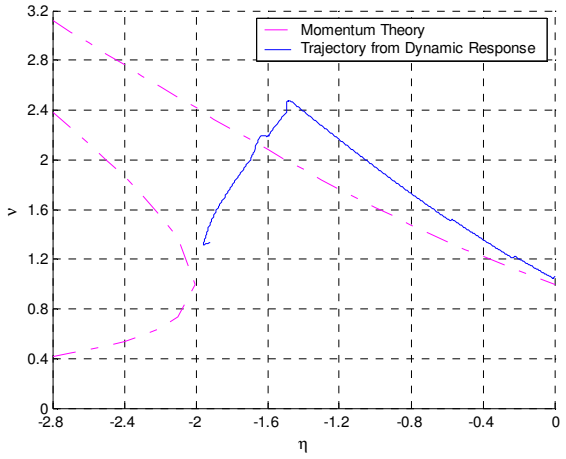

Figure 3c : Variation of Normalised Induced Velocity for Dynamic Response.

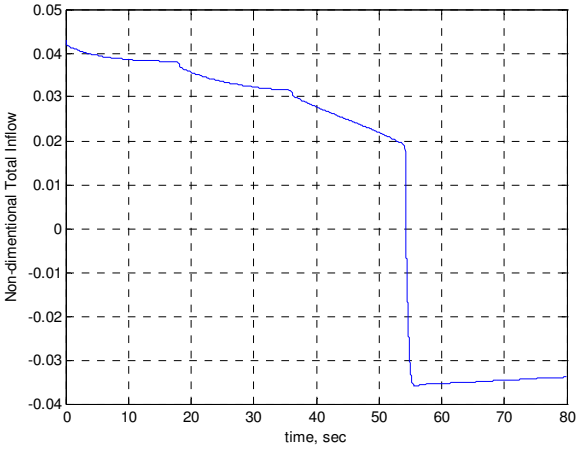

Figure 3d : Time History of Total Inflow for Dynamic Response.

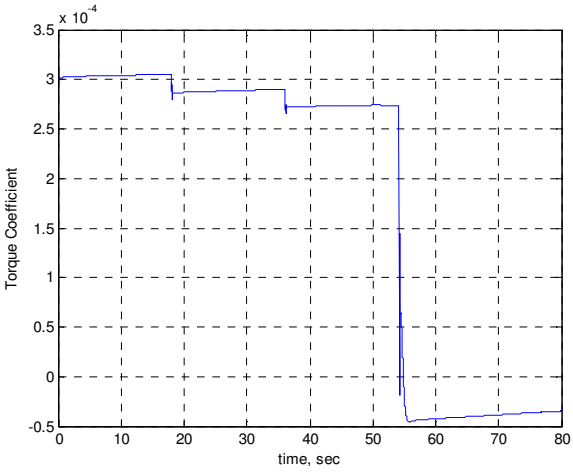

Figure 3e : Time History of Torque Coefficient for Dynamic Response.

Part 2 : Non-linear Analysis of Flight Dynamics in the VRS

Following the "Study of the VRS by bifurcation theory" initiated in (Ref. 1), Georgia Tech has carried on with the modelling problem (as presented in the first part), whereas ONERA has focused on the non-linear flight dynamics analysis.

In this second part, the rotor inflow model used for the VRS investigation is the ONERA model presented in (Refs. 8-9). This model provides a continuous solution for computing the mean inflow for any vertical and horizontal speeds combination. As shown in Fig. 4 (extract from Ref. 9) for axial descent, this extension of the momentum theory gives results which are similar with those of the vortex rings model approach presented in Part 1 (see Fig. 2a).

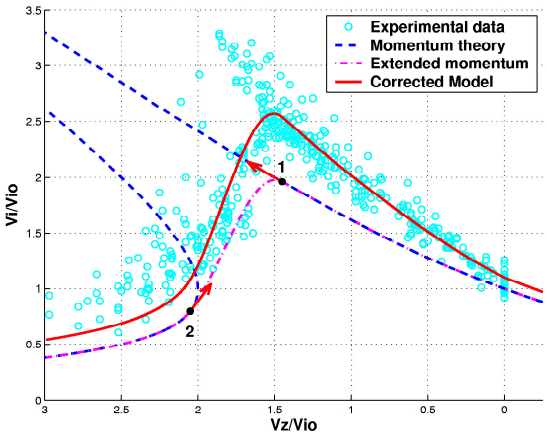

Figure 4 : ONERA mean inflow model in descents.

Nonlinear analysis methods have previously been applied to the flight dynamics problems mostly in the fixed-wing area, for example, spin motion, wing rock, air combat (Refs. 16-17). But very few examples of application to the rotorcraft flight dynamics have been published (e.g. Ref. 18, for aggressive helicopter manoeuvre and Ref. 19 for the helicopter with a slung load). However, rotorcraft flight dynamics involves various nonlinear effects coming from: e.g. individual component aerodynamics, aerodynamic interactions between components, inertial coupling, ... Moreover, the algorithms used in most of the simulation codes are, in general, inefficient in capturing all the non-linear behaviours. For example, the trim algorithms are mostly based on the Newton-Raphson method, and are, in general, not efficient in predicting possible multiple equilibrium points for the same flight condition. As an illustration of the possibility of multiple equilibrium points, a typical variation of collective pitch (DT0) required to trim a helicopter as a function of descent rate (Whel) and horizontal speed (Uhel) is shown in Figure 5. Note the fold in the equilibrium surface at low forward speed, indicating the existence of multiple equilibrium solutions, in this case three values of descent rate, for a selected value of the collective pitch.

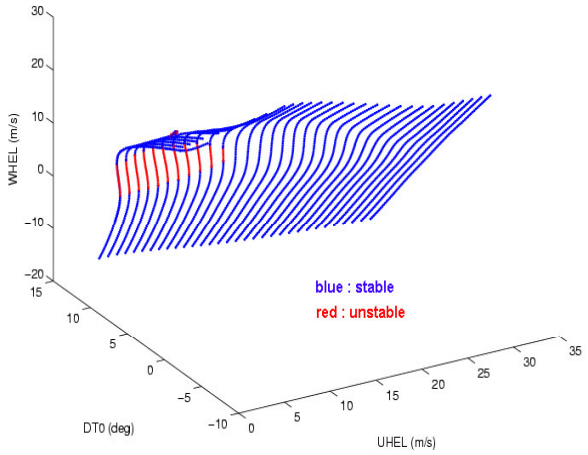

Figure 5 : Fold on the equilibrium surface.

Several non-linear analysis software tools exist, such as XppAut (including the bifurcation program AUTO) used in Ref. 1. The present study uses the non-linear analysis tool ASDOBI ("Analyse des Systèmes Différentiels Ordinaires par la méthode des BIfurcations"), a Fortran code developed by ONERA (Ref. 16-17). A first step towards the use of ASDOBI is the coupling of ASDOBI with the comprehensive rotorcraft simulation code HOST, ("Helicopter Overall Simulation Tool" created by EuroCopter and developed with contributions of ONERA Refs. 20-21). Hereafter, the minimum required mathematical background is summarised, as well as the HOST – ASDOBI coupling, in order to give the needed information for the understanding of the application to the VRS study.

Numerical treatment of the bifurcation problem

The purpose of this paper is not to describe in detail the mathematics on which the study of non-linear system dynamics are based. For example, a good presentation of bifurcation theory is provided in the books of Guckenheimer and Holmes (Ref. 22) or Iooss and Joseph (Ref. 23). The numerical aspects can be found in the book of Kubicek and Marek (e.g. Ref. 24). Hereafter only an overview of the method is presented.

Bifurcation theory concerns the behavioural changes of a dynamical system $\dot{X} = F(X,U)$ when the parameters of the system are varied, with X the state vector and U the parameter or control vector. It deals with systems governed by ordinary differential equations and focuses mainly on the asymptotic behaviour of the solutions.

Parameter values for which the system dynamics are not structurally stable are called bifurcation values, that is to say critical values such that a small parameter variation lead to qualitative changes of the trajectories of the system dynamics. Local bifurcations occur when the Jacobian matrix $D_X F(X_0,U_0) \equiv \left[\frac{\partial F_i(X_0,U_0)}{\partial x_j}\right]$ has at least one eigenvalue whose real part is zero.

Bifurcation of real or complex eigenvalues leads to different structural changes. When one real eigenvalue crosses the imaginary axis (becoming zero), there may be a creation or a destruction of some steady states. When one pair of complex eigenvalues has zero real parts, there may be a creation or a destruction of a periodic cycle (Hopf bifurcation).

Any application of the bifurcation theory to practical problems implies first to compute the steady states or equilibrium points of the model described by its differential equations. The continuation algorithm is capable of solving for the equilibrium curve even in the presence of folds or other complex patterns resulting from the non-linear terms within the system dynamics. The continuation algorithm allows the resolving of a set of equations defining an implicit solution, i.e. we are looking for the solution of $\begin{cases} \dot{x}_1 = f_1(x_1,\ldots,x_n,u) = 0 \\ \vdots \\ \dot{x}_n = f_n(x_1,\ldots,x_n,u) = 0 \end{cases}$ which is a set of n equations with $(n+1)$ variables. *(U)* the (control) parameter vector is therefore reduced to a scalar *(u)*. Let :

$$X = (x_1,\ldots,x_n), \quad F(X,u) = \begin{pmatrix} f_1(x_1,\ldots,x_n,u) \\ \vdots \\ f_n(x_1,\ldots,x_n,u) \end{pmatrix}$$

and (X_0,u_0) be a solution.

The *implicit function theorem* states that if the Jacobian matrix $D_X F(X_0,u_0)$ is non-singular, then there is a neighbourhood of the solution (X_0,u_0) on which the solutions are given by a *unique* continuous function of the parameter: $u \to (x_1,\ldots,x_n)$.

The numerical implementation of the continuation algorithm in ASDOBI allows computing the implicit solution and managing the critical points.

The algorithm is based on the repetition of four steps :

Step 1: finding a point on the equilibrium curve
Step 2: predicting the direction of the tangent
Step 3: predicting the next point
Step 4: correcting the predicted point

Step 3 is based on an Adams-Bashforth-like integrator whereas steps 1 and 4 are based on the Newton-Raphson scheme adapted to the implicit problem of *n* equations with $(n+1)$ variables.

The kind of computations which can be performed by ASDOBI are :

- locus and stability characteristics of the equilibrium points,
- equilibrium surface (set of equilibrium curves),
- locus and characteristics of real bifurcations,
- locus and characteristics of Hopf bifurcations,
- envelop of periodical orbits.

For finding bifurcation points, another equation is added in the form of $\det(D_X F(X,u_1,u_2)) = 0$ where the (control) parameter vector is a two-dimensional vector (i.e., a parameter couple for which there is a bifurcation). Thus, bifurcation points are obtained by solving the following set of $(n+1)$ equations with $(n+2)$ variables:

$$\begin{aligned} &\dot{x}_1(x_1,\ldots,x_n,u_1,u_2) = 0 \\ &\vdots \\ &\dot{x}_n(x_1,\ldots,x_n,u_1,u_2) = 0 \\ &\det(D_X F(x_1,\ldots,x_n,u_1,u_2)) = 0 \end{aligned}$$

HOST – ASDOBI Coupling

The trim option in the rotorcraft simulation code HOST is used to find a first equilibrium point (X_0,u_0) (far from suspected bifurcation points), for example hover. Then the continuation

algorithm in ASDOBI can be used to find all the equilibrium curve. Variations in the parameter vector (U) are carried out in ASDOBI while HOST provides the system dynamics. The interaction between ASDOBI and HOST is depicted in Fig. 6.

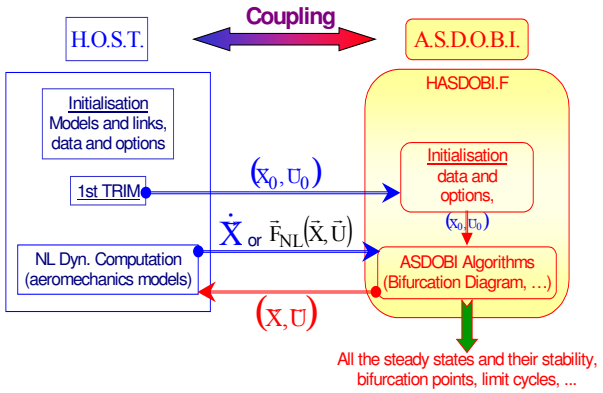

Figure 6 : HOST – ASDOBI coupling.

A validation of the integration between ASDOBI and HOST codes is carried out by comparing the trim results obtained using the HOST code alone (point by point trim with a sweep on V_z using the Newton-Raphson algorithm) and using the integrated ASDOBI – HOST code (with *DT0* as parameter in the continuation algorithm). As shown in Figure 7, the trim results are identical (within the tolerance of computational error), thus validating the integration between ASDOBI and HOST codes.

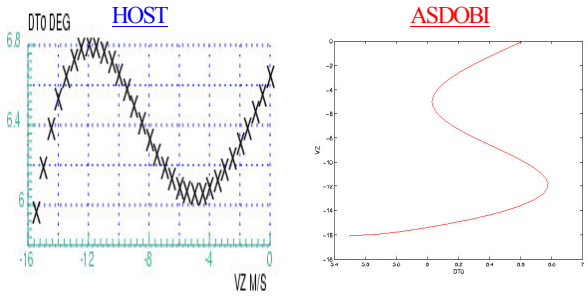

Figure 7 : Comparisons of HOST / ASDOBI trim computation.

Application to Descent Flight

As a first step, the VRS analysis has been conducted using the 'first model level' available in HOST for the Dauphin helicopter. The main rotor is represented by a rotor disk model without flapping dynamics and with the induced velocity model in the VRS developed by ONERA (Refs. 8-9).

In this model, the helicopter flight dynamics is characterised by the state variables: $X = \{U_{hel}, V_{hel}, W_{hel}, P_{hel}, Q_{hel}, R_{hel}, \phi, \theta, Vim_{MR}, Vim_{TR}\}$ (10 state variables) which involve the classical ones in aircraft flight dynamics $\{U_{hel}, V_{hel}, W_{hel}, P_{hel}, Q_{hel}, R_{hel}, \phi, \theta\}$ and the mean inflow through the main rotor and the tail rotor $\{Vim_{MR}, Vim_{TR}\}$, respectively, which are more specific to helicopter applications. The controls are $U = \{DT0, DTC, DTS, DTA\}$ (collective pitch, lateral and longitudinal cyclic pitch, tail rotor collective pitch).

Helicopter Equilibrium Calculation

The continuation algorithm works only with *one* parameter (because a numerical solution to the implicit problem is sought). The collective control *DT0* being the most important in descent flight, it has been chosen as the first critical parameter.

But in fact, when *DT0* is varied using the continuation algorithm, the other controls and parameters in the helicopter model must also vary. That is also the case for the classical point by point trim computation (by Newton – Raphson algorithm) for a sweep on flight condition (forward or descending speed for example). Hence, certain hidden constraints are implicitly used.

For example, if from a hovering flight, the collective control is decreased, then the torque of the main rotor varies, and hence, the yaw trim is no longer insured. Therefore for the study of the VRS, the yaw rate is set to zero while allowing the tail rotor collective to change. This is easily accomplished by using the algebraic equation $R_{hel} = 0$ and by freeing the *DTA* command. Thus some extra *algebraic equations* must be considered. In the case of the VRS, they are:

$$\begin{cases} R_{hel}(X, U, DTC, DTS, \mathbf{DTA}) = 0 \\ V_y(X, U, \mathbf{DTC}, DTS, DTA) = 0 \\ V_x(X, U, DTC, \mathbf{DTS}, DTA) = Const \end{cases}$$

With the above flight condition constraints, the corresponding controls are free to vary within the trim computation: the condition on the yaw rate will make mainly vary the tail collective pitch *DTA*, the condition on the lateral velocity will make mainly vary the lateral cyclic pitch *DTC* and the condition on the forward speed will make mainly vary the

longitudinal cyclic pitch *DTS*. The resulting 13 equations are:

State equations:

$\dot{X} = \{\dot{U}_{hel}, \dot{V}_{hel}, \dot{W}_{hel}, \dot{P}_{hel}, \dot{Q}_{hel}, \dot{R}_{hel}, \dot{\phi}, \dot{\theta}, \dot{V}im_{MR}, \dot{V}im_{\mathrm{TR}}\} = 0$

Constraints: $\{R_{hel}, V_y, V_x\} = \{0, 0, const\}$

and the corresponding 14 variables are:

State variables:

$X = \{U_{hel}, V_{hel}, W_{hel}, P_{hel}, Q_{hel}, R_{hel}, \phi, \theta, Vim_{MR}, Vim_{\mathrm{TR}}\}$

Control parameter: $U = \{DT0\}$

Supplementary controls: $\{DTC, DTS, DTA\}$

Figure 8 shows the equilibrium curves (with stable and unstable branches) computed by the continuation algorithm for the Dauphin helicopter in vertical descent. The stable steady states are the values towards which the helicopter is likely to stabilise whereas the unsteady ones cannot really be considered as possible flight conditions because one single perturbation makes the helicopter leave the unstable steady state, but it helps to understand the underlying dynamics.

The investigation of the VRS instabilities implies flight in a vertical plane *(x, z)* of the earth coordinate system. The relevant variables characterising the stability properties are $\{V_X, V_Z, Vim_{MR}\}$ in the earth frame, which correspond in the chosen helicopter frame to $\{U_{hel}, V_{hel}, W_{hel}, Vim_{MR}\}$. Indeed, among all the state variables characterising the helicopter flight dynamics, some variables are needed to get concrete values but don't really count much as far as stability is concerned. As a consequence, it is better to determine stability from a reduced set of state variables which are relevant from a physical viewpoint for the studied phenomenon.

Computation of the Locus of Bifurcation

As seen in the mathematical description, the bifurcation computation is performed with two control parameters, hence, only two constraints are needed instead of three. The longitudinal motion *Vx* is unconstrained and the longitudinal cyclic control *DTS* is the second control-parameter resulting in:

control parameters: $U = \{DT0, DTS\}$

algebraic equations: $\{R_{hel}, V_y\} = 0$

supplementary controls: $\{DTC, DTA\}$

The bifurcation points correspond to the values for which there is a "jump" between the helicopter and windmill stable branches. The locus computed using the integrated ASDOBI-HOST code with a 'first level model' of the Dauphin helicopter and the ONERA's VRS inflow model (Refs. 8 and 9) is compared with flight tests results in Figure 9.

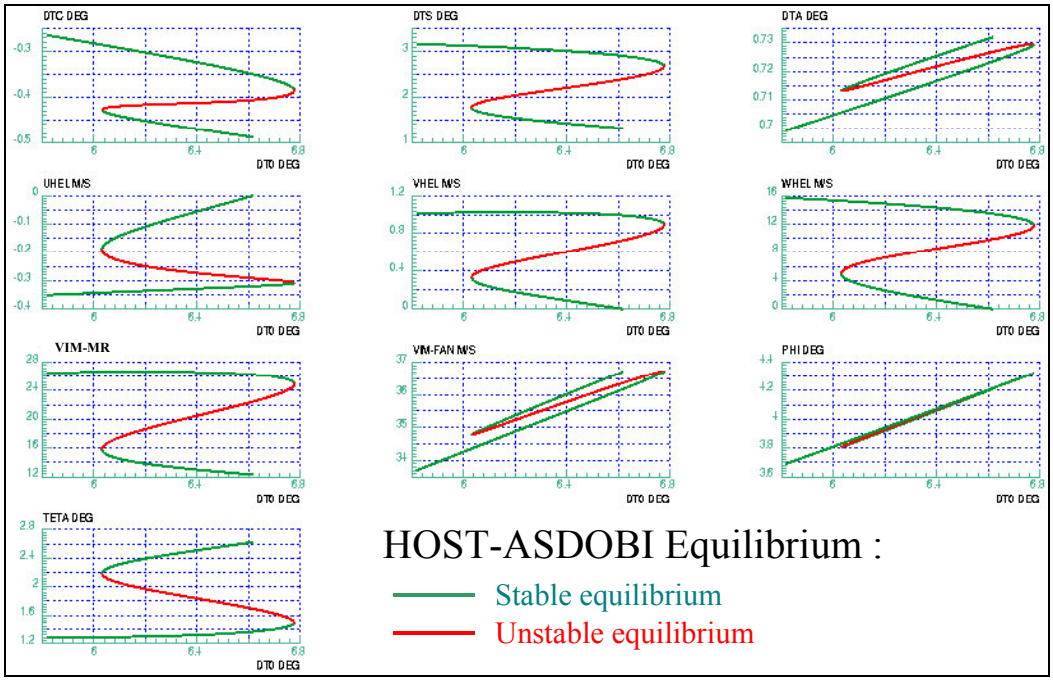

Figure 8 : Equilibrium in axial descents computed with HOST-ASDOBI (continuation algorithm on DT0).

There are two other boundaries shown in Figure 9, which are arrived at using a previously proposed criterion in the literature: the cancellation of the convection speed of the rotor tip vortices (Refs. 8-9 for the "ONERA first criterion" and Ref. 25 for the "Peters and Chen criterion").

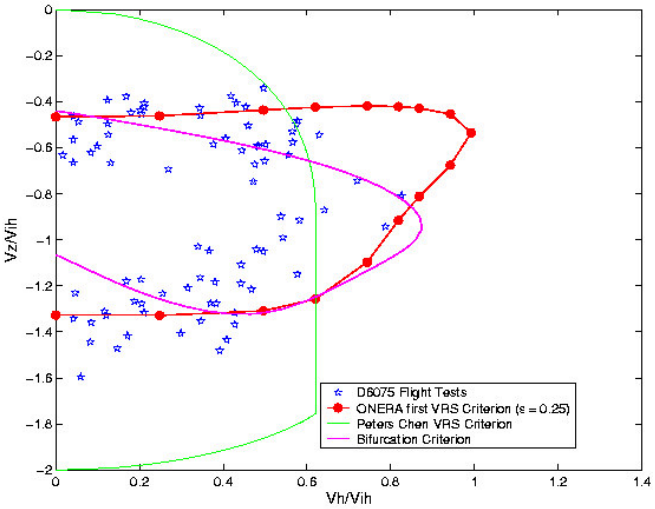

Figure 9 : VRS boundaries of the Dauphin helicopter (V_{ih} : mean inflow in hover)

The locus of the computed bifurcation points from the proposed method shown as 'Bifurcation criterion' in Figure 9, surrounds well the VRS unstable domain. One discrepancy is that the bifurcation criterion predicts a lower descent rate limit of roughly 12 m/sec (see Fig. 10) which is above the flight test data at low forward speed.

In fact, as illustrated in Figure 10, the HOST-ASDOBI results highlight that the bifurcation from the wind-mill branch to the helicopter branch occurs for lower descent rates. The flight tests were done from the helicopter regime. Hence, the "Vz stabilization" points correspond to higher descent rates on the wind-mill branch. Thus the flight test results show the 'exit of the VRS' from the helicopter branch, whereas the bifurcation criterion reveals the 'entry into the VRS' from the windmill branch.

Model Sensitivity of the Bifurcation Locus

The ONERA VRS model (Refs. 8-9), adds an extra induced velocity to the momentum theory value, similar to the vortex rings model (Ref. 13) presented in Part 1, to account for the increase of downwash due to the interaction with the vortex wake coming closer to the rotor. Also, similar to the vortex rings model of Part 1, the ONERA VRS inflow model exhibits nonlinear behaviour with descent rate.

In order to study the influence of the nonlinear behaviour of the induced velocity model on the VRS boundaries prediction, the curvature of the extra downwash ("expo" parameter) is varied, getting a family of curves shown in Figure 11 for example in axial descent. The resulting variation in the total flow through the rotor in vertical descent is shown in Figure 12. As a consequence, the collective pitch needed to create the adequate thrust for trimming the helicopter in axial descent is different as shown in Figure 13.

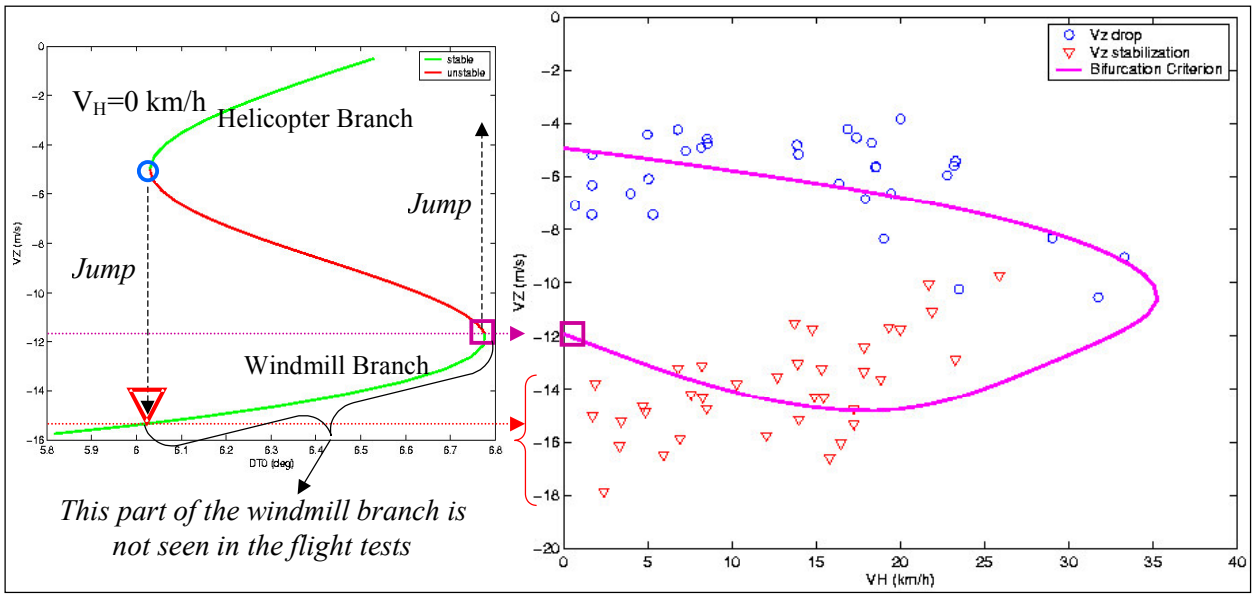

Figure 10 : The bifurcations from the windmill branch ("square") are not caught in the flight test.

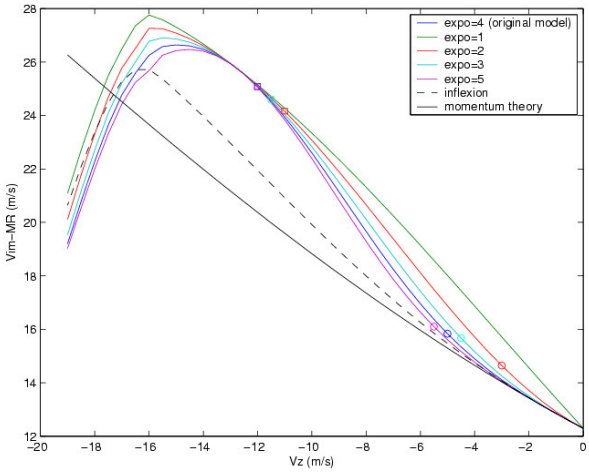

Figure 11 : Effect of model variations on the mean induced flow in axial descent.

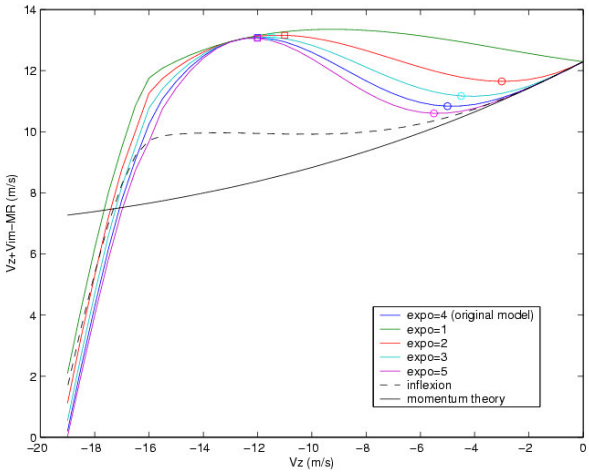

Figure 12 : Total mean flow through the rotor in axial descent.

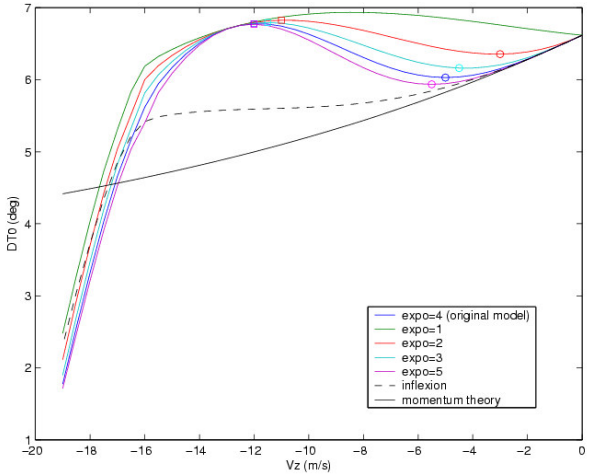

Figure 13 : Effect of model variation on trim collective in axial descent.

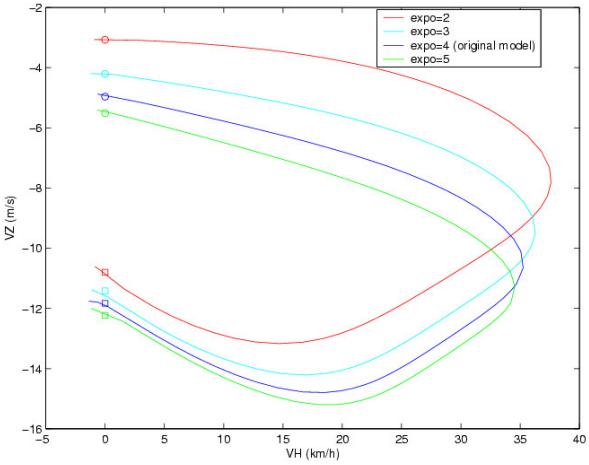

Figure 14 : Effect of model variation on VRS boundary.

The corresponding effect on the complete locus of the bifurcation points surrounding the VRS region, is shown in Fig. 14 in the plane *(Vx=V_H, Vz).* The results shown in Fig. 9 with the original inflow model (Refs. 8-9) correspond to the curves with "expo = 4" in Fig. 14.

The circles and squares are the bifurcation points in axial descent. The circles on these figures are the bifurcations from the helicopter branch (low descent rates), and the squares are the bifurcations from the windmill branch (high descent rates). The parts between these symbols shown on the curves of Figures 11-13 are unstable equilibrium. For a small perturbation of the collective control *(DT0)* from a steady-state close to these bifurcation points, the rotorcraft state will quickly transition toward the other stable branch leading to a significant change in the vertical speed *(Vz).* Except for the curves obtained with the "momentum theory", "expo=1" and "inflexion", there are three equilibrium points for the range of *(DT0)* between the bifurcation points as can be seen in Figure 13. The model with "expo=1" is not physically representative since it predicts that the trim collective must increase for very low descent rates right from hover. The part of the "expo=1" curve between hover and the maximum of *DT0* is unstable.

The results shown in Figures 11 through 14 may be used to postulate the following requirements on the rotor inflow model to represent the VRS instabilities. First, a requirement for the existence of the VRS unstable region is that there must exist two points at which $d(V_z + Vim_{MR})/dV_z = 0$ (see Figure 12), which is equivalent to saying that there must exit two points at which $(dVim_{MR}/dV_z = -1)$

(see Fig. 11). Second, these two points are separated by an inflexion point $\left(d^2 Vim_{MR} / dV_z{}^2 = 0\right)$ such that the corresponding points in Figures 12 and 13 are a minimum and a maximum. More precisely, the bifurcation for the low descent rate (bifurcation from the helicopter branch) must be a minimum of $(Vz+Vim_{MR}) = f(Vz)$ and the other must be a maximum. Physically speaking, a rotorcraft will encounter the VRS from the helicopter mode when by decreasing the collective, it will reach a local minimum (shown by a circle on Figure 13) of the equilibrium curve (*Vz, DT0)*. By continuing to decrease *DT0*, it will enter the VRS and then stabilise at a higher descent rate on the windmill branch.

Hence, from a modelling point of view, the model with "expo=1" leads to a wrong VRS prediction because the curve $(Vim_{MR}=f(Vz))$ does not exhibit an inflexion point. The curve noted "inflexion", although it has an inflexion point, will also not represent the VRS because it does not have two points with the required slope: $\left(dVim_{MR} / dV_z = -1\right)$.

Therefore, it is not sufficient for a model to predict an increase of the downwash over the one given by the momentum theory (see the cases of "expo = 1" and "inflexion"). The increase of the mean inflow in descent flight must be non-linear in such a way that :

- on the helicopter branch (from hover until the circles) : *dVim < -dVz*
- at the bifurcation noted by a circle: *dVim = -dVz*
- between the two bifurcation (circle and square) : *dVim > -dVz*
- at the bifurcation noted by a square : *dVim = -dVz*
- then: *dVim<-dVz* until (*Vim)* reaches a maximum and then decreases with the increasing descent rate.

It is important to note that some of the above requirements are similar to those described in Refs. 12-13, arrived at by considering the heave stability.

From the physics point of view, this non-linear increase of *(Vim)* with the descent rate (in addition to the increase predicted by the momentum theory) is probably due to different phenomena. The mean convection airspeed $(Vz+Vim_{MR})$ of the vortex layers generated by the rotor must have a non-linear variation in descent. But the geometrical explanation of the increase of downwash by the fact that the vortices are coming closer to the rotor may not be the only reason. It can be noticed in the experimental data (see Fig. 4) as well as in the ONERA model (Figures 4 and 11) that the maximum of mean induced flow *(Vim)* is not reached for $(Vz+Vim_{MR}) = 0$. The induced flow at the rotor level increases not only with the decreasing distance between the vortices and the rotor disk, but also with their vortex strengths which may also have a non-linear variation with the descent rate.

Conclusions

Recent results from an on-going cooperation between ONERA and the Georgia Institute of Technology on rotor inflow modelling and analysis during descent flight including the VRS are presented as two parts. In the first part, results from a validation study of the vortex rings model developed in Ref. 13 are given. It is shown that vortex rings along the wake at rotor periphery induce additional downward velocities at the rotor disk. The magnitude of the additional part of the induced velocity reaches a point where higher sink rate requires larger collective pitch for trim. The steeper gradient of the ν-η curve from the vortex rings model gives rise to a reversal in the heave damping for a range of descent rates. Validation results show good correlations between predictions from the vortex rings model and wind tunnel experimental data.

In the second part, a methodology based on the bifurcation theory for analysis of the helicopter non-linear flight dynamics in the VRS is described. Results from an application of the methodology for prediction of the VRS boundaries are compared with Dauphin helicopter flight test data. An important result is that the VRS unstable region is well surrounded by the prediction given by the locus of the bifurcation points of the system dynamics in descent flight. Using results from a model sensitivity study, it is shown that the additional downwash (over the momentum theory prediction) from the VRS inflow model must exhibit certain nonlinear characteristics with descent rate for a good prediction of the VRS boundaries.

Acknowledgements

This study was conducted under the cooperation established between ONERA and the Georgia Institute of Technology as part of the US-France MoA task on rotorcraft flight dynamics. The second author would like to acknowledge the financial support from the DSO National Laboratories, Singapore, for his graduate study program at Georgia Tech.

References

[1] Basset, P.-M., and Prasad, J.V.R., "Study of the Vortex Ring State Using Bifurcation Theory", American Helicopter Society 58th Annual Forum, Montréal, Canada, June 11-13, 2002.

[2] Castles, W. Jr., and Gray, R.B., "Empirical Relation Between Induced Velocity, Thrust, and Rate of Descent of a Helicopter Rotor as Determined by Wind-Tunnel Tests on Four Model Rotors", NACA TN 2474, October 1951.

[3] Wolkovitch, J. "Analytic Prediction of Vortex-Ring Boundaries for Helicopters in Steep Descents", Journal of the American Helicopter Society, Vol. 17, No. 3, July 1971.

[4] Wang, S.C., "Analytical Approach to the Induced Flow of a Helicopter Rotor in Vertical Descent", Journal of the American Helicopter Society, January, 1990.

[5] Leishman, J.G., Bhagwat, M.J., and Ananthan S., "Free-Vortex Wake Predictions of the Vortex Ring State for Single-Rotor and Multi-Rotor Configurations", American Helicopter Society 58th Annual Forum, Montréal, Canada, June 11-13, 2002.

[6] Glauert, H., "The Analysis of Experimental Results in the Windmill Bake and Vortex Ring States of an Airscrew", R. & M. No. 1026, British A.R.C., 1926.

[7] He, C.J., Lee, C.S., Chen, W.B., "Finite State Induced Flow Model in Vortex Ring State", American Helicopter Society 55th Annual Forum, Montréal, Canada, May 25-27, 1999.

[8] Jimenez, "Experimental and Numerical Study of the Helicopter Behaviour in Steep Descent and Modelling of the Vortex Ring State", PhD Thesis, ONERA, 2002.

[9] Jimenez, Desopper, Taghizad, Binet, *"Induced Velocity Model in Steep Descent and Vortex-Ring State Prediction"*, 27th European Rotorcraft Forum Proceedings, Moscow, Russia, 2001.

[10] Taghizad, A., Jimenez, J., Binet, L, and Heuzé, D., "Experimental and Theoretical Investigation to Develop a Model of Rotor Aerodynamics Adapted to Steep Descent", American Helicopter Society 58th Annual Forum, Montréal, Canada, June 11-13, 2002.

[11] Taghizad, Jimenez, Arnaud, "Helicopter Flight Tests in Steep Descent : Vortex-Ring State Analysis and Induced Velocity Models Improvements", CEAS/TRA3 Conference proceedings, Cambridge (UK), 2002.

[12] Johnson, W., "Model for Vortex Ring State Influence on Rotorcraft Flight Dynamics", AHS 4th Decennial Specialist's Conference on Aeromechanics, San Francisco, California, January 21-23, 2004.

[13] Chen, C., Prasad, J.V.R., and Basset, P.M., "A Simplified Inflow Model of a Helicopter Rotor in Vertical Descent", American Helicopter Society 60th Annual Forum, Baltimore, MD, June 7-10, 2004.

[14] Castles, W., and Leeuw, J.H., "The Normal Component of the Induced Velocity in the Vicinity of a Lifting Rotor and Some Examples of its Application", NACA TN 2912, 1953.

[15] Advance Rotorcraft Technology, Inc., "FLIGHTLAB Theory Manual", April 2001.

[16] Guicheteau, P., "Bifurcation theory : a tool for nonlinear flight dynamics", Phil. Trans. R. Soc. Lond. A, 1998.

[17] Guicheteau, P., "Stability Analysis through Bifurcation Theory" and "Non-Linear Flight Dynamics", AGARD Lecture series 191, Non Linear Dynamics and Chaos, 1993.

[18] Sibilski, "Bifurcation Analysis of a Helicopter Non-Linear Dynamics", 24th European Rotorcraft Forum, Marseilles, France, 1998.

[19] Sibilski, "Prediction of Critical Configurations of Helicopter External Slung Load System Using Bifurcation Theory and Continuation Methods", Journal of Theoretical and Applied Mechanics, n° 4, Vol. 41, 2003.

[20] Benoit, B., Dequin, A.-M., Basset, P.-M., Gimonet, B., Grünhagen, W. von, Kampa, K., "HOST, a General Helicopter Simulation Tool for Germany and France", American Helicopter Society 56th Annual Forum, Virginia Beach, Virginia, May 2 – 4, 2000.

[21] Basset, P.-M., El Omary, A., "A rotor vortex wake model for helicopter flight mechanics and its application to the prediction of the pitch-up phenomenon", 25th European Rotorcraft Forum Rome, Italy, September 14-16, 1999.

[22] Guckenheimer, Holmes, "Nonlinear Oscillations, Dynamical Systems, and Bifurcations of Vector Fields", Springer Verlag, 1983-1996.

[23] Iooss, Joseph, "Elementary Stability and Bifurcation Theory", Springer Verlag, 1980.

[24] Kubicek, Marek, "Computational Methods in Bifurcation Theory and Dissipative Structures", Springer Verlag, 1983.

[25] Peters, D.A., Chen, S.Y., "Momentum Theory, Dynamic Inflow, and the Vortex Rings State", Vol. 28, No. 3, Journal of The American Helicopter Society, July 1982.